11th World Congress on Computational Mechanics (WCCM XI)
5th European Conference on Computational Mechanics (ECCM V)
6th European Conference on Computational Fluid Dynamics (ECFD VI)
E. Oñate, J. Oliver and A. Huerta (Eds)

CAPTURING AEROSOL DROPLET NUCLEATION AND CONDENSATION BURSTS USING PISO AND TVD SCHEMES

E.M.A. Frederix[1], A.K. Kuczaj[3,1], M. Nordlund[3] and B.J. Geurts[1,2]

[1]Multiscale Modeling and Simulation, Faculty EEMCS, J.M. Burgers Center, University of Twente, P.O. Box 217, 7500 AE Enschede, The Netherlands, e.m.a.frederix@utwente.nl
[2] Anisotropic Turbulence, Fluid Dynamics Laboratory, Faculty of Applied Physics, Eindhoven University of Technology, P.O. Box 513, 5600 MB Eindhoven, The Netherlands
[3] Philip Morris International R&D, Philip Morris Products S.A., Quai Jeanrenaud 5, 2000 Neuchatel, Switzerland

Key words: PISO, aerosol, nucleation, compressible flow, grid refinement, TVD schemes

Abstract. A mathematical model for single-species aerosol production and transport is formulated, and solved using an adapted PISO algorithm. The model is applied to a laminar flow diffusion chamber, using a finite volume method on a collocated grid. In transient simulations, a sharp scalar front (e.g., vapor mass fraction), is shown to introduce unphysical oscillation in the solution, when applying a second order linear interpolation in the convective terms. At increased grid resolution, these oscillations are strongly attenuated. When applying a TVD scheme (here the MUSCL scheme), a time-accurate monotonicity-preserving solution is obtained. The numerical dissipation introduced by the MUSCL scheme implies increased spatial resolution to restore high accuracy levels. We develop a one-dimensional grid refinement algorithm, which relates the grid density in one direction to the magnitude of the scalar gradient. In combination with the MUSCL scheme, this gives accurate results, with a significant reduction in computational effort, in comparison with a uniform fine grid.

1 INTRODUCTION

The formation of an aerosol is a complex physical phenomenon. Although an aerosol is often perceived as a uniform gaseous substance, it contains many small dispersed droplets or particles. The scales which govern the evolution of such an aerosol are not only macroscopic. For example, the interaction of individual molecules in a supersaturated vapor determines the homogeneous nucleation rate, which, in turn, defines macroscopic properties of the aerosol, such as composition or surface deposition rate.

To describe the microscopic physics of aerosol formation using macroscopic quantities, classical nucleation theory (CNT) [1] is adopted. CNT is sensitive to mixture properties

such as temperature and saturation. Variation in pressure or temperature may lead to a critically supersaturated state and results in rapid bursts of newly created aerosol droplets. Condensation of vapor onto these droplets subsequently decreases the saturation, thereby effectively stopping further nucleation. In the modeling of multiphase fluid flow, the occurrence of nucleation and condensation puts a stringent requirement on the accuracy of the numerical method. First, the environment in which nucleation is triggered should be well captured by the method. Moreover, the sharp gradients in the solution associated with nucleation, call for accurate numerical treatment.

In this work, a numerical study of a single-species two-moment Eulerian aerosol model [2] in a finite volume framework is presented. The model is applied to describe aerosol formation, evolution and transport in a laminar flow diffusion chamber (LFDC), as designed by Nguyen et al. [3]. In an LFDC a saturated vapor flows into a cooled pipe. The vapor obtains a critically supersaturated state, leading to nucleation and subsequent aerosol droplet growth by condensation. The LFDC is used to experimentally determine a nucleation rate, and its dependence on operational parameters, e.g., the flow rate and temperature gradient. In our model, the aerosol which is formed in the LFDC is characterized in terms of two moments [4]: a mass fraction and droplet number concentration. Droplets are created through nucleation, as described by CNT. Vapor to aerosol mass transport occurs through both nucleation and condensation. Along with an inert carrier gas, the vapor and aerosol are part of a compressible mixture, in view of density variations due to phase transitions and temperature gradients. Therefore, the mass, momentum and energy conservation equations are solved in their compressible forms. This approach is required, since the large LFDC temperature gradient introduces equivalently large gradients in density.

The conservation equations are solved by adopting the compressible PISO algorithm as proposed by Issa [5] and Issa et al. [6]. In the literature there is sufficient evidence to claim that the PISO algorithm is efficient, robust, accurate and versatile (e.g., [7, 8, 9, 10]). The extension of the compressible PISO algorithm for reacting flows [6] was mainly applied to combustion problems (e.g., [6, 11, 12, 13]). Here, we apply the PISO algorithm to the modeling of single-species aerosol nucleation, evolution and transport in laminar flow.

Typically, the region in which nucleation occurs is small. Therefore, in a transient simulation, a very sharp aerosol front is generated, which is convected in the domain. When employing a second order central discretization scheme for the convective term of the aerosol moment transport equations, unphysical numerical oscillations are introduced near the aerosol front. These oscillations decay slowly in time, while being advected out of the flow domain. In this work, we present and compare two methods which address this problem. First, we show that employing the MUSCL TVD interpolation scheme [14] to the scalar convection terms preserves the monotonicity of the solution and yields a time-accurate transient solution, free of unphysical oscillations, on any grid resolution studied. Second, we show for the central discretization scheme employing linear interpolation instead of MUSCL interpolation, that with increased grid resolution the amplitude of the

numerical oscillations decrease. We introduce an efficient and robust one-dimensional grid refinement method, which relates the grid density to the magnitude of the scalar gradient. In this way, using a relatively small amount of grid cells, numerical oscillations as seen in the central discretization approach approach may also be suppressed. Moreover, in combination with the MUSCL scheme, an accurate solution is obtained, with a significantly reduced computational cost.

The organization of this paper is as follows. First, in section 2 we introduce the model and briefly describe the adapted PISO algorithm. In section 3 the grid refinement method is discussed. Finally, in section 4 the two proposed methods, i.e., the application of the MUSCL scheme and the grid refinement method, are compared. Conclusions are given in section 5.

2 SINGLE-SPECIES AEROSOL MODEL AND NUMERICAL ALGORITHM

In this section we discuss the conservative equations for mass, momentum and energy, governing a mixture of inert carrier gas, vapor and aerosol. The single-species aerosol is characterized using two moments: the aerosol mass fraction and the droplet number concentration. For the description of droplet production, we adopt CNT, relating the nucleation rate of droplets to macroscopic properties of the mixture. We solve the mass and momentum equations in a segregated way, following closely the *Pressure-Implicit with Splitting of Operators* (PISO) method [6] for reacting flows.

2.1 Single-species two-moment aerosol model

Following [2] and [15], the compressible conservative equations for mass, momentum and energy may be formulated as

$$\partial_t \rho + \nabla \cdot (\rho \boldsymbol{u}) = 0 \tag{1a}$$

$$\partial_t (\rho \boldsymbol{u}) + \nabla \cdot (\rho \boldsymbol{u}\boldsymbol{u}) = -\nabla p + \nabla \cdot (\mu \boldsymbol{\tau}) \tag{1b}$$

$$c_p \partial_t (\rho T) + c_p \nabla \cdot (\rho T \boldsymbol{u}) = \nabla \cdot (k \nabla T) + \mu \boldsymbol{\tau} (\nabla \boldsymbol{u}) + D_t p, \tag{1c}$$

with velocity $\boldsymbol{u}$, mixture density ρ, pressure p and material derivative D_t. The energy equation is formulated in terms of temperature T. The equations (1) are valid for a mixture, such that the specific heat at constant pressure c_p, thermal conductivity k and dynamic viscosity μ are effective mixture properties. We use a mass fraction-weighted averaging of the corresponding specific properties, to compute the effective values. For the rate of strain tensor $\boldsymbol{\tau}$, we use that of a compressible Newtonian fluid.

The mixture is constituted of three mass fractions, i.e., vapor mass fraction Y, aerosol mass fraction Z and inert carrier gas mass fraction Y_0. By definition the sum of these three quantities is equal to unity. For each mass fraction a conservative transport equation

is formulated:

$$\partial_t(\rho Y_0) + \nabla \cdot (\rho Y_0 \boldsymbol{u}) = \nabla \cdot (\rho D \nabla Y_0) \tag{2a}$$
$$\partial_t(\rho Y) + \nabla \cdot (\rho Y \boldsymbol{u}) = \nabla \cdot (\rho D \nabla Y) + S_{l\to v} \tag{2b}$$
$$\partial_t(\rho Z) + \nabla \cdot (\rho Z \boldsymbol{u}) = -S_{l\to v}, \tag{2c}$$

where $S_{l\to v}$ is a source term which enables vapor-aerosol mass transport, and D is the binary diffusivity of vapor in carrier gas. These three equations are not consistent with (1a), as the diffusive fluxes of vapor and carrier gas do not necessarily cancel. However, since the vapor mass fraction is generally small, the error as a result of this inconsistency is negligible. In stead of replacing one equation in (2c) with $Y_0 + Y + Z = 1$, we solve each equation in (2c), such that error is not absorbed by only one mass fraction. The aerosol, consisting of relatively immobile droplets, is assumed to have a negligible diffusion. Along with mass fraction Z, we describe the aerosol with a second moment, i.e., the droplet number concentration N. Analogous to (2c) a conservation equation may be formulated for N:

$$\partial_t N + \nabla \cdot (N \boldsymbol{u}) = J_{nuc}, \tag{3}$$

in which the source term $J_{nuc} \geq 0$ appears, which governs the production of droplets by means of nucleation. It is assumed in (3) that droplet coalescence or breakup does not occur.

The set of equations (1), (2) and (3) is closed using an equation of state, relating the mixture density to pressure via compressibility ψ. The compressibility may, in turn, depend on pressure or temperature:

$$\rho = \psi(p, T)p. \tag{4}$$

The compressibility is a mass fraction-weighted average of the corresponding specific compressibilities.

2.2 Aerosol nucleation and condensation source terms

In a supersaturated vapor mixture, due to the rapid motion of vapor molecules, small clusters are formed. These clusters may grow through collisions with free moving molecules, or they may shrink in size as trapped molecules 'escape', i.e., evaporate. There exists a so-called *critical cluster* of vapor molecules, which has an equal probability of either growing or disappearing. The CNT is concerned with such a critical cluster, and relates the nucleation rate to the probability of critical cluster formation. Following [2] and [16], the effective form of the nucleation rate is given by

$$J_{nuc} = 3^{1/3}\sqrt{\frac{\sigma}{m\pi}}\left(\frac{p_v}{k_B T}\right)^2 V_m \exp\left(-\frac{16\pi\sigma^3 V_m^2}{3k_B^3 T^3 \log^2 S}\right), \tag{5}$$

which is derived under the assumption that the volume of a critical cluster is much larger than that of an individual molecule. In (5), σ is the condensed species bulk surface

tension, m the molecular mass, p_v the vapor pressure, k_B Boltzmann's constant, V_m the molecular volume and S the saturation ratio.

Along with the formation of droplets, vapor mass is transformed intro liquid. When droplets are nucleated, they have a radius corresponding to that of the critical cluster. This radius is given with the Kelvin equation, i.e.,

$$r^* = \frac{2\sigma V_m}{k_B T \log S}, \tag{6}$$

in which ρ_l is the liquid mass density of the aerosol. The mass transport as a result of nucleation is therefore given by

$$S_{nuc} = \frac{4}{3}\pi (r^*)^2 \rho_l J_{nuc}. \tag{7}$$

Again following [2], the mass flow rate as a result of evaporation or condensation, is modeled with (also see [17]):

$$S_{e-c} = 4\pi \left(\frac{3\rho Z}{\pi \rho_l N}\right)^{1/3} \exp\left(-\log^2 W\right) D\rho(1-Z) \log\left(\frac{1-Y}{1-Y_s}\right) N, \tag{8}$$

with W the geometric standard deviation of the particle size distribution (here assumed to be $W = 4/3$, see [18]), vapor diffusivity D and saturation mass fraction Y_s. Using equations (7) and (8), the total liquid to vapor mass transfer rate becomes:

$$S_{l\to v} = -S_{nuc} + S_{e-c}. \tag{9}$$

2.3 Numerical method

To solve the coupled set of equations, we closely follow the PISO algorithm for reacting flows [6]. Whereas the original PISO algorithm is formulated for scalar transport in a combustion problem, we adapt the algorithm such that equations (2) and (3) are incorporated. Each term is discretized using a finite volume method on a collocated grid, meaning that each solution variable is only defined and stored at cell centers. The segregated solution approach of PISO, in combination with a collocated grid, is known to lead to pressure-velocity decoupling and unphysical pressure and velocity fluctuations. For this reason, we apply Rhie-Chow interpolation [19] for the computation of the velocity at cell interfaces. For the discretization of the partial time derivatives, we employ the Crank-Nicolson scheme. The PISO scheme takes, while following the notation in Ref. [6], the following form:

1. Implicit predictor equations are solved to find $\boldsymbol{u}^*$, T^*, Y_0^*, Y^*, Z^* and N^*. Based on this, a prediction is found for the compressibility, i.e., ψ^*.

2. The Poisson-like pressure equation is solved to obtain a corrected pressure p^* and a corresponding corrected density ρ^*. Using these two corrected fields, a corrected velocity $\boldsymbol{u}^{**}$ is obtained. The momentum flux at cell faces is corrected using p^*, in agreement with Rhie-Chow interpolation.

3. Using this corrected momentum flux, corrected temperature, mass fractions and droplet number concentrations are found at time level $**$. Based on these solutions the source terms may be re-evaluated.

4. Given the updated solutions for velocity, temperature, etc, the pressure p^* does not necessarily satisfy an updated pressure equation. Step 2 and 3 are repeated until the splitting error is sufficiently converged towards zero. We measure the convergence by considering the initial residual of the updated pressure equation, using the latest pressure.

5. When convergence is achieved, the generally temperature-dependent mixture coefficients μ, k, etc, are updated. Steps 1-5 are repeated for a new time step.

3 ADAPTIVE GRID ALGORITHM

In a transient LFDC simulation, at $t = 0$ a saturated vapor is injected into a laminar pipe flow. This vapor front has a sharp gradient in terms of mass fraction Y. In the collocated finite volume method treatment of the convective term, Y must be interpolated to the cell faces. Using a linear second order interpolation scheme, numerical oscillations are introduced near a sharp scalar front, as the value of the interpolated mass fraction may vary significantly from the cell centered one. These oscillations disappear when the vapor front is accurately resolved with an adequate grid resolution. In our grid refinement approach, we relate the grid density to the magnitude of the vapor gradient, such that at locations with a large vapor gradient the typical grid cell size is small.

Let us consider a one-dimensional profile $\phi(x)$ corresponding to for example the vapor mass fraction Y averaged over the LFDC pipe cross section. The profile is scaled such that $-\frac{1}{2} \leq \phi(x) \leq \frac{1}{2}$. We update the x distribution of grid points every time interval τ, according to the x-direction non-uniform grid density P. The function P relates the grid point density to the magnitude of the scalar gradient, such that a large gradient corresponds to a high grid density. P is defined as:

$$P = q\left\{1 + \frac{a}{2}\left(|\partial_x \phi(x)| + |\partial_x \phi(x - \tau U)|\right)\right\}, \tag{10}$$

with U the velocity of the vapor front. The parameter a controls how strong the grid density depends on the magnitude of the gradient. The second spatial derivative in the right-hand side of (10) accounts for the fact that in time interval τ, the front has traveled a distance of τU. We found that the addition of this term significantly improved the

method, in terms of oscillation suppression. The parameter q can be found using

$$\int_0^L P \mathrm{d}x = M - 1, \tag{11}$$

where it is assumed that the computational domain is bounded by $0 \leq x \leq L$, and M is the number of grid points in x-direction. Relation (11) guarantees that M grid points are distributed over the domain. In general (11) must be evaluated numerically, since ϕ is only known at M grid points at position x_i with $1 \leq i \leq M$. Alternatively, for stability, we may also fit a continuously differentiable function to ϕ, such that the spatial derivative of ϕ is known at any point x. In the case of a vapor front, a hyperbolic tangent is fit to ϕ, using a least squares method. We find each new grid cell position x_i^* from

$$x_i^* = x_{i-1}^* + P(x_i^*)^{-1}. \tag{12}$$

We iteratively solve this recursion relation by setting $x_1^* = 0$ and solving for x_2^* using Newton iteration, and so on. Since ϕ is approximated with a continuously differentiable function, P can in general be evaluated at any point. This improves the stability of the method. The point x_M^* is in general close, but not equal to L. We therefore scale as a final step each x_i^* using

$$x_i := x_i^* \frac{L}{x_M^*}, \tag{13}$$

which guarantees that $x_M^* = L$.

Given a new grid distribution in x-direction, a new computational grid is generated. Each solution field is interpolated to this grid, using a trilinear interpolation scheme, and the PISO algorithm may be continued for a next time step on this new grid.

4 NUMERICAL RESULTS

We consider the 'system B' LFDC of Nguyen et al. [3]. Because of symmetry, we only simulate a two-dimensional wedge with a computational grid of N_x cells in the axial direction and N_r cells in radial direction. On the pipe wall a temperature profile is specified using a Dirichlet boundary condition, which mimics the measured one reported in [3]. As an inlet condition, a Poiseuille velocity profile is specified, while setting the vapor mass fraction to that at saturation. The drop in temperature leads to a rise in saturation, which, in turn, triggers the nucleation. In a relatively small zone, particles are nucleated. Through condensation, the remaining vapor is transformed into liquid droplets.

In a transient simulation, a vapor front is rapidly cooled, and condenses into an aerosol front. Figure 1 shows the pipe centerline solution for N, for 5 consecutive time steps. It is shown that on a coarse grid numerical oscillations occur near the aerosol front, when employing a second order linear interpolation scheme to the convective term. On a fine grid, these oscillations are suppressed. It is also shown that as $t \to \infty$, the oscillations are

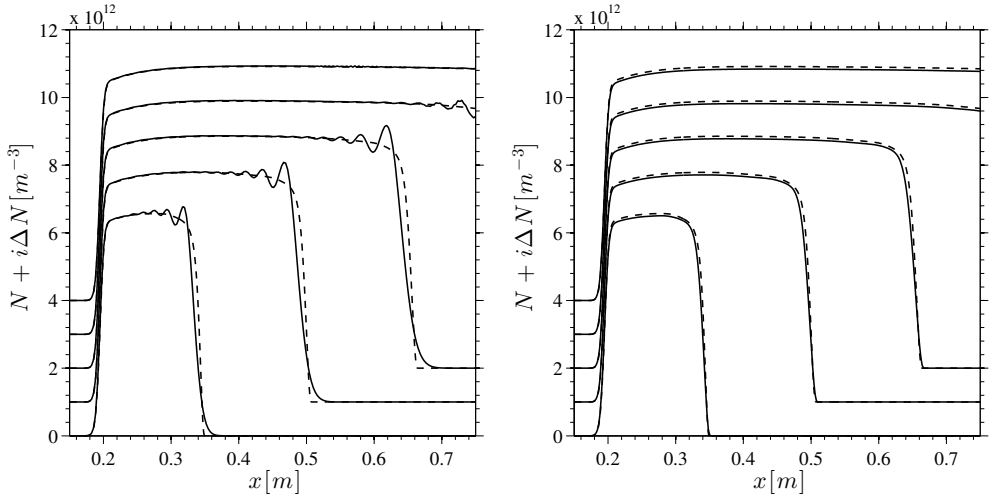

Figure 1: Centerline transient solutions for the droplet number concentration N, for five consecutive times (each separated with an offset of $\Delta N = 10^{12}$). Figure (a) shows the results for a linear interpolation scheme applied to the convective term in the N transport equation, for an $N_x = 256$ by $N_r = 16$ grid (solid line) and an $N_x = 1024$ by $N_r = 64$ grid (dashed line). Figure (b) shows the results for the MUSCL TVD interpolation scheme an $N_x = 256$ by $N_r = 16$ grid (solid line), and the same dashed line as in figure (a).

convected out of the computational domain. When using the MUSCL scheme, a coarse grid gives time-accurate results, without numerical oscillations.

As a simple test case, we simulate the transport of a saturated vapor front through the LFDC, at constant temperature, i.e., no condensation occurs. In this way we may analyze the convective treatment of a sharp scalar front. At $t = 0$ the vapor is injected. As the front advances through the pipe, it is smeared out as a result of diffusivity. Figure 2 shows for four different simulations the centerline profile for Y, at $t = 2$. It is shown that on a coarse grid ($N_r = 8$, $N_x = 128$) using a linear interpolation scheme, the solution for Y shows large differences with respect to the solution on a fine grid ($N_r = 8$, $N_x = 3072$). Using the MUSCL scheme, on a coarse grid a time-accurate solution is shown, which preserves the monotonicity of the solution. However, large over- and underestimations of the solution are shown in front and behind the front in case of modest local resolution of the sharp gradient. Applying the adaptive grid algorithm to the coarse grid, in combination with the MUSCL scheme, significantly improves the accuracy of the solution, and a good agreement is shown with the fine grid solution. In comparison with the fine grid solution, 24 times less grid cells were used, resulting in a comparable factor of reduction in computational cost, for an equal and constant time step size.

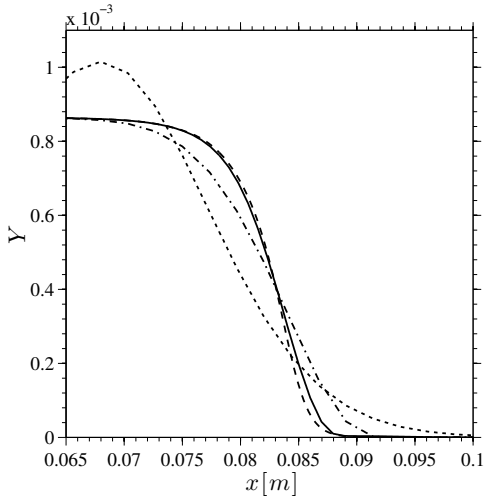

Figure 2: Solutions for the vapor mass fraction front on a coarse grid, using a central discretization with linear interpolation (dotted), on a coarse grid using MUSCL (dash-dotted), on a coarse grid using MUSCL and grid refinement (solid) and on a fine grid (dashed).

5 CONCLUSIONS

In this paper we discussed the formulation of a mathematical model for single-species aerosol formation, using a two-moment approach. The PISO algorithm was used to solve the model, in a segregated way, using a finite volume method on a collocated grid. It was shown that in transient aerosol formation simulations, sharp spatial fronts in vapor and aerosol mass fractions, or droplet number concentration, lead to unphysical oscillations in the corresponding solutions, when employing linear interpolation in the convective terms. For an increased grid resolution, these oscillations are suppressed. Also, using a TVD interpolation scheme (e.g., MUSCL), it is shown that on coarse grids time-accurate monotonicity-preserving solutions are found. However, these solution are less accurate than the fine grid ones. We introduced, in addition, a one-dimensional grid refinement approach, which locally refines the grid near (and in front of) a scalar front. The grid density is related to the magnitude of the gradient of the scalar field. It was shown that this approach, in combination with the MUSCL scheme, on coarse grids yields accurate solutions, in comparison with fine grid ones, while the decrease in computational cost is, for a constant time step, proportional to the decrease in grid density.

ACKNOWLEDGEMENTS

The research described in this paper was supported by Philip Morris Products S.A. and the authors wish to thank Philip Morris Products S.A. for their financial support.

REFERENCES

[1] R. Becker and W. Döring, "Kinetische Behandlung der Keimbildung in übersättigten Dämpfen," *Annalen der Physik*, vol. 416, no. 8, pp. 719–752, 1935.

[2] C. Winkelmann, M. Nordlund, A. Kuczaj, S. Stolz, and B. Geurts, "Efficient second-order time integration for single-species aerosol formation and evolution," *International Journal for Numerical Methods in Fluids*, vol. 74, no. 5, pp. 313–334, 2014.

[3] H. Nguyen, K. Okuyama, T. Mimura, Y. Kousaka, R. Flagan, and J. Seinfeld, "Homogeneous and heterogeneous nucleation in a laminar flow aerosol generator," *Journal of Colloid and Interface Science*, vol. 119, no. 2, pp. 491–504, 1987.

[4] M. Frenklach and S. J. Harris, "Aerosol dynamics modeling using the method of moments," *Journal of Colloid and Interface Science*, vol. 118, no. 1, pp. 252–261, 1987.

[5] R. Issa, "Solution of the implicitly discretised fluid flow equations by operator-splitting," *Journal of Computational Physics*, vol. 62, no. 1, pp. 40–65, 1986.

[6] R. Issa, B. Ahmadi-Befrui, K. Beshay, and A. Gosman, "Solution of the implicitly discretised reacting flow equations by operator-splitting," *Journal of Computational Physics*, vol. 93, no. 2, pp. 388–410, 1991.

[7] R. Issa, A. Gosman, and A. Watkins, "The computation of compressible and incompressible recirculating flows by a non-iterative implicit scheme," *Journal of Computational Physics*, vol. 62, no. 1, pp. 66–82, 1986.

[8] N. Bressloff, "A parallel pressure implicit splitting of operators algorithm applied to flows at all speeds," *International Journal for Numerical Methods in Fluids*, vol. 36, no. 5, pp. 497–518, 2001.

[9] I. E. Barton, "Comparison of SIMPLE- and PISO-type algorithms for transient flows," *International Journal for Numerical Methods in Fluids*, vol. 26, no. 4, pp. 459–483, 1998.

[10] A. Wanik and U. Schnell, "Some remarks on the PISO and SIMPLE algorithms for steady turbulent flow problems," *Computers and Fluids*, vol. 17, no. 4, pp. 555–570, 1989.

[11] D. M. Wang, A. P. Watkins, and R. S. Cant, "Three-dimensional diesel engine combustion simulation with a modified EPISO procedure," *Numerical Heat Transfer, Part A: Applications*, vol. 24, no. 3, pp. 249–272, 1993.

[12] D. Wang and A. Watkins, "Numerical modeling of diesel spray wall impaction phenomena," *International Journal of Heat and Fluid Flow*, vol. 14, no. 3, pp. 301–312, 1993.

[13] W. Chow and N. Fong, "Application of field modelling technique to simulate interaction of sprinkler and fire-induced smoke layer," *Combustion Science and Technology*, vol. 89, no. 1-4, pp. 101–151, 1993.

[14] B. van Leer, "Towards the ultimate conservative difference scheme. V. A second-order sequel to Godunov's method," *Journal of Computational Physics*, vol. 32, no. 1, pp. 101–136, 1979.

[15] R. B. Bird, W. E. Stewart, and E. N. Lightfoot, *Transport Phenomena*. John Wiley & Sons, Inc., second ed., 2007.

[16] H. Vehkamäki, *Classical Nucleation Theory in Multicomponent Systems*. Springer, 2006.

[17] S. Friedlander, *Smoke, Dust, and Haze: Fundamentals of Aerosol Dynamics*. Oxford University Press, 2nd ed., 2000.

[18] W. Hinds, *Aerosol Technology*. John Wiley & Sons, Inc., second ed., 1999.

[19] C. Rhie and W. Chow, "Numerical study of the turbulent flow past an airfoil with trailing edge separation," *AIAA Journal*, vol. 21, no. 11, pp. 1525–1532, 1983.